

Structural health monitoring based on static measurements with temperature compensation

Viet Ha Nguyen¹, Sebastian Schommer¹, Arno Zürbes², Stefan Maas¹

¹ *University of Luxembourg, Faculty of Science, Technology and Communication, Research Unit Engineering Sciences, Rue Coudenhove–Kalergi 6; L – 1359 Luxembourg*
² *Fachhochschule Bingen, Fachbereich 2 - Technik, Informatik und Wirtschaft, Germany*

E-mails: ¹vietha.nguyen@uni.lu

Abstract

The paper presents the main results from static tests in a prestressed concrete beam taken out from a real bridge. The tests were achieved during about one month with several scenarios of damage that loaded and unloaded states were monitored for each scenario. Damages in 4 levels were simulated by cutting prestressed tendons. There were 8 transducers distributed along the length's beam to measure displacements.

Deflection lines resulted from the static measurements from every state allow discovering the location of damages. Moreover, the calculation of slope and curvature lines leads also to very interesting issues for damage localization.

Keywords: bridge, localization, damage, displacement, temperature

1 Introduction

Damage detection for mechanical systems during their life-cycle has been studied and developed a lot these last decades. The most of research consists in analyzing dynamic characteristics, namely modal features like eigenfrequencies, mode shapes or damping ratios. The modal features may be used for other procedures like model updating, stiffness/flexibility assessment, sensitivity analysis... to localize and assess damage (Reynders & De Roeck, 2010; Huth et al., 2005; Nguyen & Golinval, 2010), even to predict remaining life (Khan et al., 2015). On the other hand, static load tests providing important information on deformation, displacement, tilt and strain (Inaudi, 2010) are still an appropriate alternative that the measurements are easy. Moreover, a direct correlation between these quantities and temperature variation can be drawn up when the effect of temperature is of interest.

Recently, having an opportunity to examine a part of a real prestressed concrete bridge, the Research Unit in Engineering Sciences - University of Luxembourg has analyzed both static and dynamic responses. The structure was monitored during its initial condition and 4 different damaged states. In the present paper, only the analysis of static measurements is presented. Some discussions are also revealed on the whole process of static tests during the monitoring.

2 Description of the structure

2.1 Situation of the testing beam

It consists in a bridge built between 1953 and 1955, which crossed Mosel River between Luxembourg and Germany. It was demolished in 2013 and replaced by a steel bridge. The old bridge had 5 independent fields, each consisted of 5 parallel prestressed concrete beams, which carried the driving lane. Further to the demolition, two of these beams that the length is of 46 m and the mass is of about 120 tons were shipped to the nearby port of Merttert for the test purposes.

The idea is to simulate the situation during the life of bridge and then measure structural responses. So one of the beams was used to make up a simply supported beam model, as shown in Figure 1. The fix and sliding bearings were realized onto the nearby railroads, which have a solid concrete foundation. On this existing foundation, firstly two blocks were made by cast-in-place concrete. Secondly, the beam was lifted onto these blocks by a crane. At the fixed end of the beam, movement in any direction was impossible. For the sliding bearing, two steel plates were placed between the beam and the concrete block. The friction between the two plates was reduced by grease so that the beam could slide on these plates. In fact, this was not a perfect sliding bearing because some friction may still exist between the plates. However, longitudinal movement in the beam, for example due to thermal expansion, were also feasible.

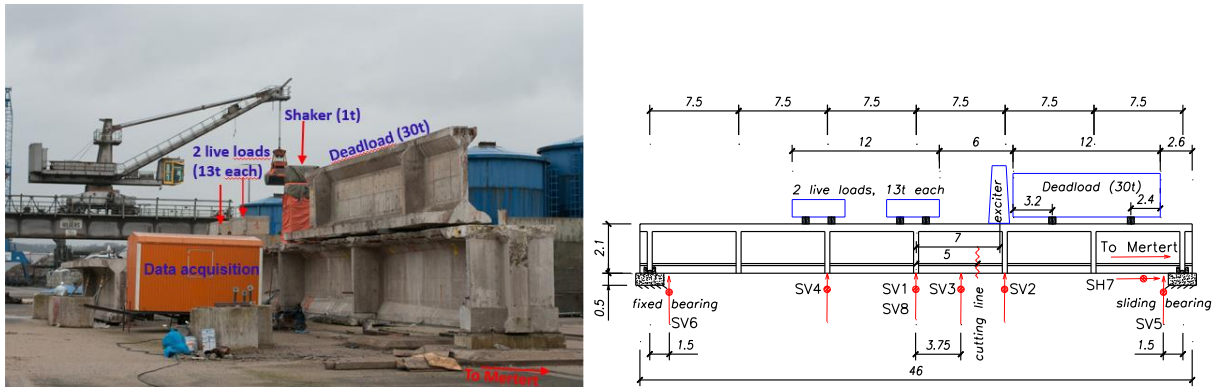


Figure 1 : Test set up - Configuration of the beam and positions of transducers for static measurements

During the bridge’s lifetime, the beams had not only to carry themselves but also the traffic lane (asphalt layer), sidewalk and other additions. Hence, even without traffic, the permanent load was higher than in the test set-up so far. So to simulate this additional dead load, a part of the second beam with a mass of approximately 30t was set on the top of structure. This mass stayed onto the beam during the whole test period and is therefore referred to permanent load. Although it was not distributed over the whole beam like an asphalt layer, it was considered as an admissible approximation.

Additionally, two concrete blocks, each with a mass of 13t, were used to represent live loads due to high traffic loading on the bridge. They were put on for static tests and removed again after at least 24 hours. Displacements were recorded in several locations, as detailed in Figure 1, along the vertical (SV1-SV6, SV8) and horizontal directions (SH7). The static test lasted one month.

Transducer SH7 was placed near the sliding bearing to verify the horizontal movement of this bearing. By putting vertical transducers more abundant, it is expected that the fact may give interesting information about changes in static deflection of the beam, especially in damaged states. The transducers were placed to measure in the middle of the cross-section, except SV1 and SV8. These two transducers are both in the midmost of the beam length but measure for two opposing sides of the web for assessing the beam’s inclination.

2.2 Damage scenarios

The beam was prestressed by 19 steel tendons along the longitudinal direction of the beam. They are illustrated in Figure 2 for a half of the beam. This figure shows also the cross-section of some tendons that each tendon was composed of 12 steel fibres with a diameter of 7 mm.

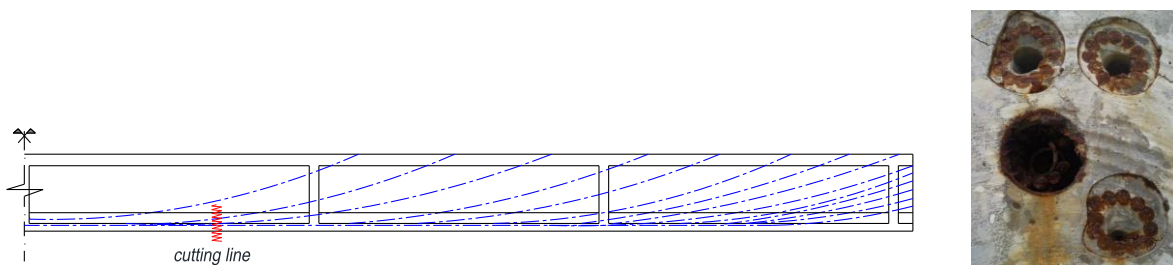


Figure 2 : Disposition of tendons shown in a half of the beam’s length and cross-section of some tendons

Different damage scenarios were simulated by cutting the tendons at the cutting line indicated in Figures 1 and 2. The position of the tendons according to the cutting line is reflected in Figure 3 with the lower part of the beam’s cross-section. A whitening of a tendon represents its cutting. The initial state #0 and other four damages #1 to #4 are reported in Table 1. Within each damage state, the tendons were cut symmetrically in the cross-section. For damages #1 to #3, the tendons were perfectly cut because they were all in the outer layer of tendons, which could be uncovered just after removing the concrete cover. However, for the last damage, tendons were only partially damaged because the inner layer of tendons could not be completely cut; it was too hard to be achieved without removing much more surrounding concrete. Consequently, only half of the fibres were cut for each tendon in the inner layer, as illustrated in Figure 3 for damage #4. The situation of cutting and cracking are also reported there.



Figure 3: Cutting of tendons in all the damage scenarios and Cracks observed in damage scenario #4

Table 1: Damage scenarios

State	Cutting of	Observation on crack
#0	0 tendon	
#1	2 tendons	Horizontal cracks appear near the cut tendons due to shear stress by cause of friction in the tendons when new anchorages were made by the cut.
#2	4 tendons	Extension of horizontal cracks
#3	6 tendons	First vertical cracks, above the cutting line; extension of horizontal cracks
#4	6 tendons+ half of 6 others tendons	More vertical cracks near the cutting line; extension of existing cracks

3 Data processing

3.1 Overall measured displacements

Besides the permanent monitoring by the 8 transducers, another alternative performed for static test was optical measurement. It lasted during more than 2 hours that compared 8 points of reference (near the bearings and in the middle of the beam) between before and after loading. The optical results showed that the displacement errors are small.

Displacements shown in Figure 4 distinguish clearly two principal situations: loading (L) and unloading (UL). A loading is performed by putting the two weights of 13 tons each on the top of the beam as indicated in Figure 1. Among the total 9 loadings, the first two times are considered as test-only to stabilize the system; only 7 times are examined: #0-L1; #0-L2; #1-L; #2-L; #3-L; #4-L1 and #4-L2.

The static displacements gives important information for damage localization, especially from the evolution of vertical displacement measured from SV3 and SV2, which are adjoining to the cutting line (see Figure 1). Let us consider Figure 4 that reports the complete static loading test for every damage state. Before damage #3, SV1 and SV8 locating in the middle of the beam show the highest values; but from #3 (6th February), SV3 rose up and went over SV1/SV8; SV2 went over SV4. The raising of displacements in SV2, SV3 corresponds really to the opening of cracks between these transducers, therefore this is an efficient way to localize the damage.

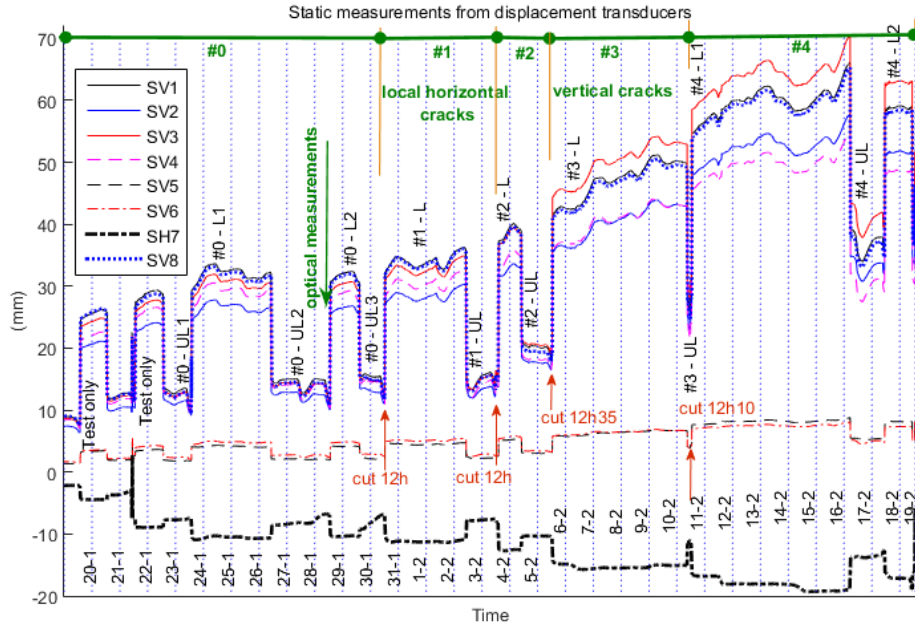


Figure 4 : Static measurements from transducers for 7 vertical and 1 horizontal displacements

Another phenomenon can be observed in damage #4 that there were two loadings in this state. It shows a clear diminution of displacement from the first loading #4-L1 to the second #4-L2. Actually, this concerns a residual deformation that was revealed in (Waltering, 2009) when considering a simple beam supporting a concentrated load in the middle of the span and different damage scenarios. As interpreted in Figure 5a, during a loading, the deformations comprised two steps: elastic and plastic (the OA and AB segment respectively). However after the unloading (the BC segment), the beam did not return to its configuration before the loading, i.e. it exists always a residual deformation (OC). That may concern namely plasticity, cracking, creeping... effects. But a 2nd or 3rd/4th loading from C would follow the line CB.

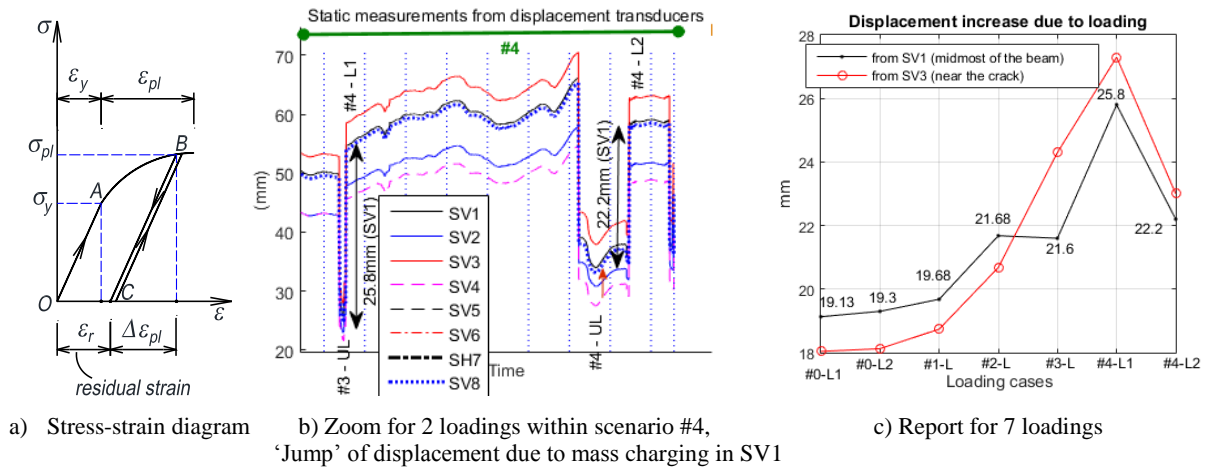
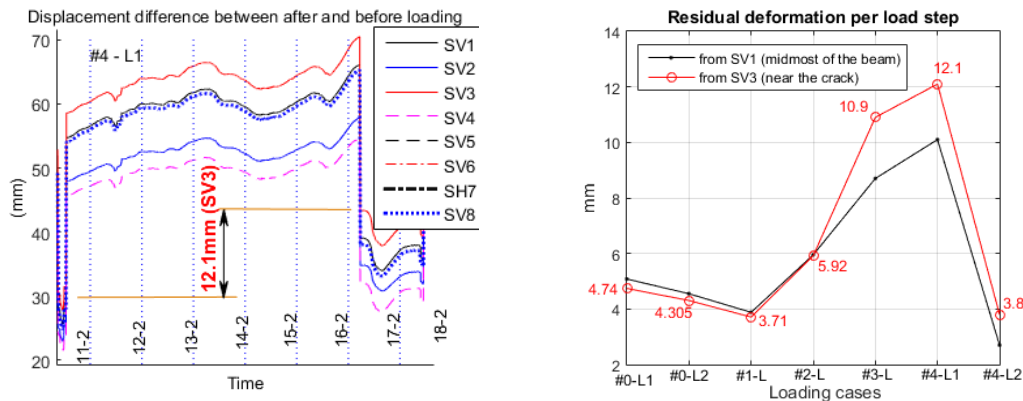


Figure 5 : (a) Stress-strain diagram; (b and c) 'Jump' of displacement due to mass charging

Therefore, let us return to the present work, it is worth examining the last loading #4-L2 on 18-19/2, this is the second loading during damage scenario #4 that the displacements are clearly lower than the first loading #4-L1 of the same damage scenario. Figure 5b;c investigates the increase in displacements due to each loading by comparing the difference between just after and before putting on the live loads. The records show a considerable drop of displacement increase within the last loading. By comparison with the precedent loading #4-L1 (from 11/2 to 17/2), a high diminution is revealed: SV1 in the middle was increased by 25.8mm due to loading #4-L1 and by only 22.2mm for loading #4-L2. It is assumed that during the first loading of scenario #4 (#4-L1), the structure underwent considerable plastic deformations (that were well observed in (Waltering, 2009), revealed here in Figure 5a). The bridge was then unloaded (from 17/2 to 18/2) and residual deformations were still staying and thus they

had been (or nearly) excluded from the following loading. It could be the reason that the second loading of state #4 (#4-L2) shows a decrease of displacement. Therefore, this last loading reflects much better the displacement increasing due to only the charging of the masses. A report for the all 7 times of loading is subsequently given in Figure 5b.



a) Zoom for the 1st loading in scenario #4 (#4-L1), residual deformation in SV3 is 12.1mm

b) Report for 7 loadings

Figure 6: Remaining displacements after each loading

To have a look on the residual deformation due to creeping, plastification... in the examined structure, Figure 6 presents the difference of displacements according to each loading. They are computed from the displacements measured just before putting masses and the displacements recorded when the masses are already removed, as illustrated in Figure 6a. No studying yet on the origin of these remaining displacements, Figure 6b shows clearly that the strong increase according to SV3, which passes over SV1 in scenarios #3 and #4, allows localizing the damage. The localization is evident because SV1 is in the middle of the beam, normally among all the transducers, SV1 corresponds to the highest deflection; however SV3 was very close to the cutting line then its measurements overcame SV1. Similar localization by SV3 may be also detected from Figure 5b.

Another aspect is revealed from Figure 5b, that the second loading of state #4 (#4-L2) shows a reduction of deflection with respect to the first loading of #4. It relies on permanent deformation after the first loading in a state. Therefore, the second loading in each state may concern principally the elastic deformation due to the charging without (or very little) the plastic or irreversible part. Unfortunately, we did not carry out the re-loading in cases of damage states #1, #2, #3 for removing the plastification and cracking deformation in each damage state. Attention should be paid for works in the future that re-loading should be performed for every condition. For each damage scenarios, it is necessary to do at least 2 subsequent loadings and use the second to eliminate the plasticity and cracking effect, which might be present extensively in the first loading.

3.2 Deflection curve and its derivatives

The aim here is to establish deflection lines of the beam, distinguished from zero position of reference configuration. Since the first two loadings in Figure 4 were used just for stabilizing the system, the data are analysed only after these two loadings. While static measurements had started up already before, on 22-1 some transducers were rearranged. This time is then considered as a new starting point, we introduced an offset for every transducer, so that their values were started from zero there. The sake of this offset is to approach the first unloaded, undamaged state and the no-deformed shape of the beam.

Figure 7 presents deflection lines of the beam for both unloading and loading states by connecting simply measured points SV1 to SV6. Two zero points are assigned according to the two border bearings. The data are picked up according to 8 unloading times and 7 loading times from scenario #0 to #4. Before the appearance of vertical cracks, the deflection curves are quite regular in an overall view. After that, a breaking point and maximum deflection are clearly shown in SV3, which is close to the cutting line and not in SV1, despite that SV1 is in the midmost of the beam. It proves that the drawing of deflection curves from the initial state to all the damage states allows localizing accurately the damage.

For a comparison, the deflection lines are also smoothed out through the cubic spline interpolation. This interpolation assures the continuity of the first and second derivatives of the spline at the measurement points. Other boundary conditions are at the two extremity points (bearings), the second derivative is adopted by zero value. The interpolation results are presented in Figure 8.

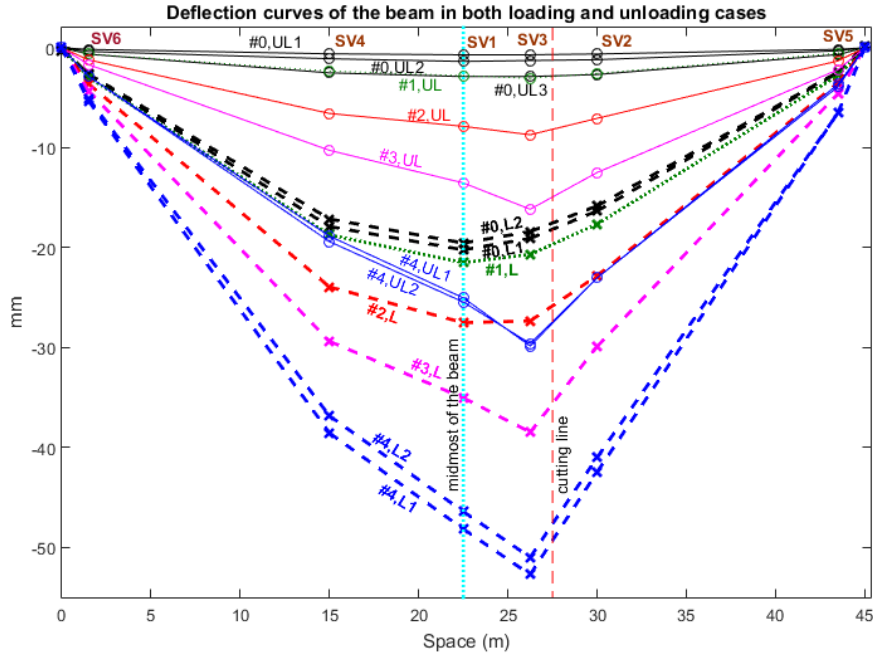


Figure 7 : Deflection of the beam in unloaded and loaded states

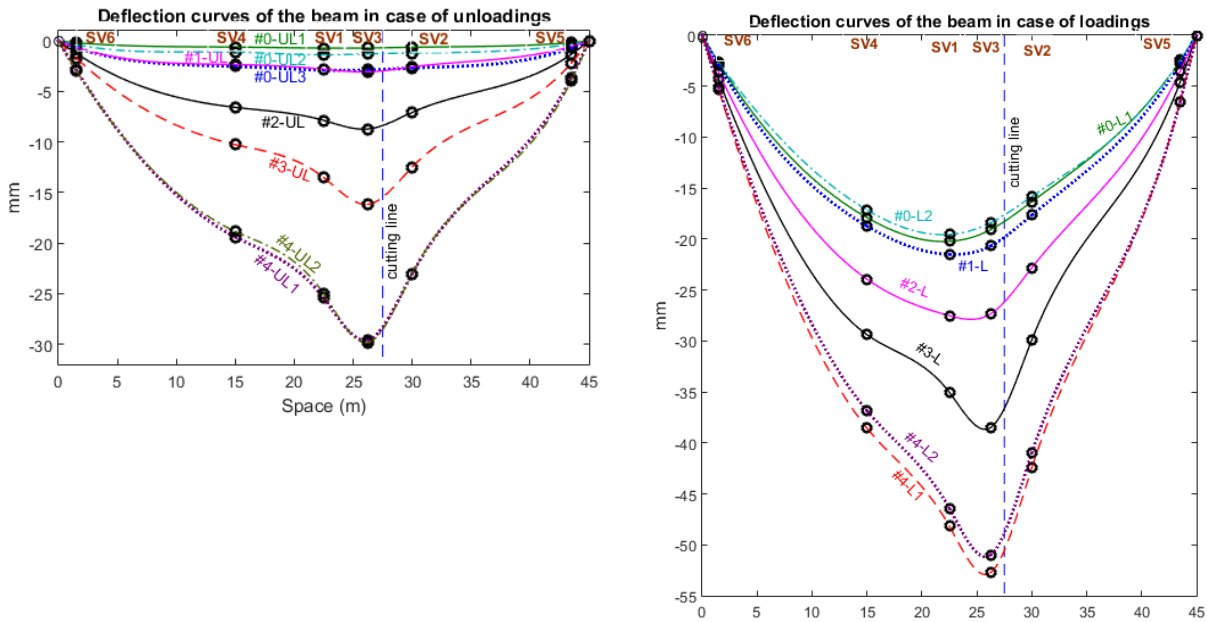


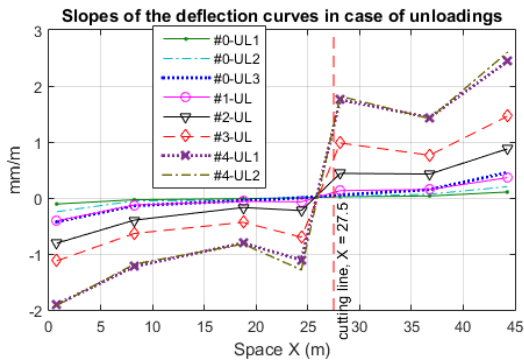
Figure 8 : Deflection of the beam in unloaded and loaded states by cubic spline interpolation

While damages are detected by breaking points in the raw deflection lines in Figure 7, they are localized by important change of shape and the increase in displacement near the cutting line. The absolute values in Figures 7-8 can be used also as damage indicator. Looking at only loaded or unloaded state, near the crack (SV3), at least 30mm were finally distinguished from the healthy reference state. This very important value indicates as well the presence of damage.

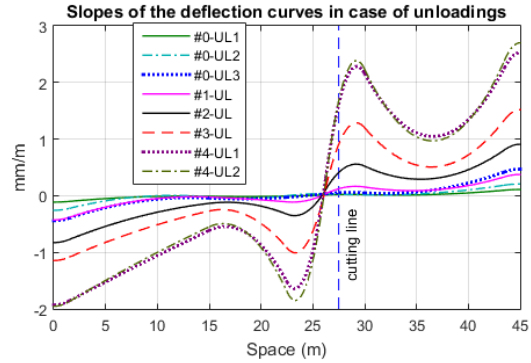
Table 2: Distinction between the two types of deflection lines

	From the raw deflection lines	From the spline deflection lines
Deflection line	Links 8 points: SV1 to SV6 + 2 boundary zero points (1)	Cubic spline interpolated from 8 points (cited in the left column) (2)

1 st derivative / Slope	7 points, $w'_i = \frac{w_i - w_{i-1}}{x_i - x_{i-1}}$ at abscise $\frac{x_i + x_{i-1}}{2}$ (3) The first point is located between the first (fixed) bearing and SV6, the last point is between the second (sliding) bearing and SV5.	Derivative from (2) - polynomial of degree 2 (4)
2 nd derivative / Curvature	6 points, $w''_i = \frac{w'_{i+1} - w'_i}{\frac{x_{i+1} + x_{i+1}}{2} - \frac{x_{i-1} + x_i}{2}} = \frac{w'_{i+1} - w'_i}{\frac{x_{i+1} - x_{i-1}}{2}}$ (5) at abscise $\frac{x_{i-1} + 2x_i + x_{i+1}}{4}$	Derivative from (4) - polynomial of degree 1 (linear) (6)



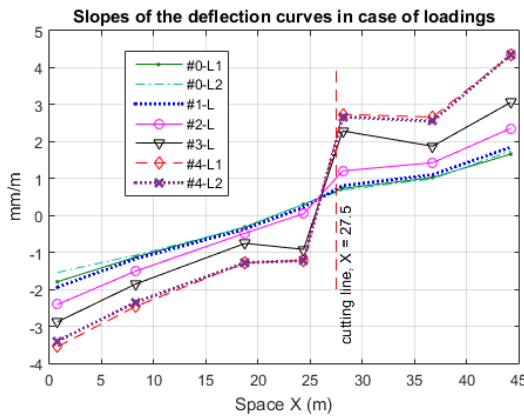
a) From the raw deflection line – (3) in Table 2



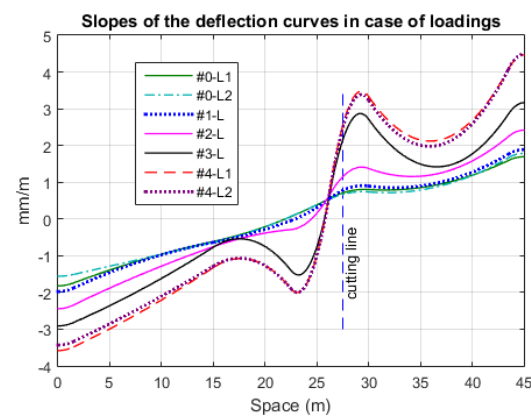
b) From the cubic spline deflection line- (4) in Table 2

Figure 9 : Slopes for unloaded states

Naturally, the derivatives of the deflection curves namely slope and curvature should be explicitly helpful for the localization. The first derivative (slope) is shown in Figure 9 for the unloaded states according to both the raw deflections and the smooth curves from interpolation. The difference between the two ways is further outlined in Table 2.



a) From the raw deflection line- (3) in Table 2

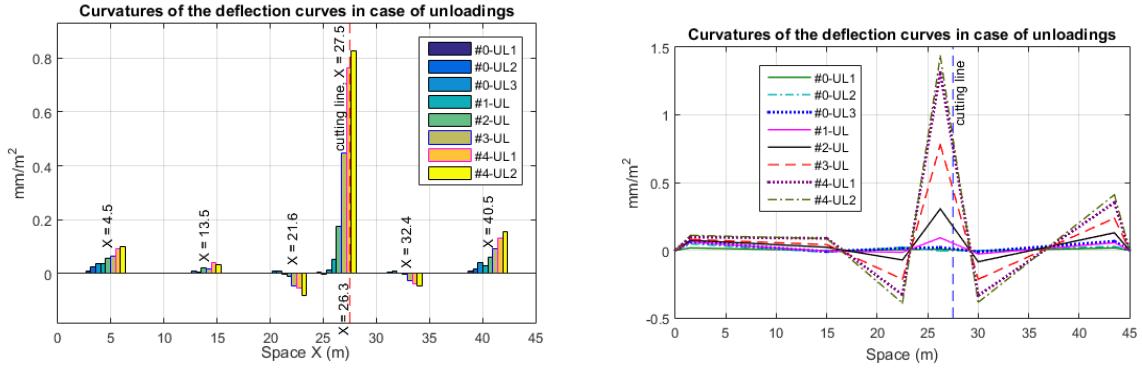


b) from the cubic spline deflection line- (4) in Table 2

Figure 10 : Slopes for loaded states

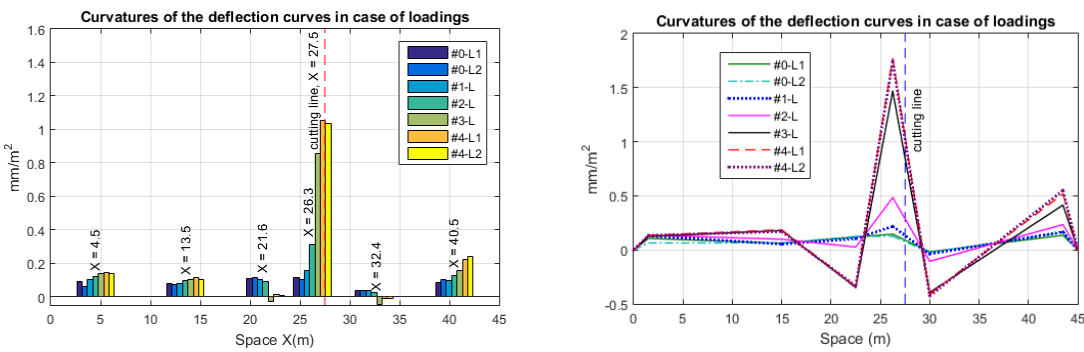
Firstly, based on the raw deflection lines, damage can be identified by strong variation of the slopes around the cutting line in image (a) of Figures 9;10 for unloaded and loaded states respectively. This strong variation leads to high values of curvatures near the cutting line, as shown in image a) of Figures 11-12. Damages are accurately localized as the curvatures near the cutting line show dominant values against other positions, from unloaded to loaded states.

From the raw deflection lines, the curvatures are computed and indicated with according abscissae. The curvatures reveal clearly surpassing values at abscissa $x=26.3m$, near the cutting line while other positions in the beam obtain similar trivial values. It shows that the damage localization is efficient and accurate from damage state #2, not only for loaded states but also for unloaded states.



a) From the raw deflection lines – Eq.(5) in Table 2 b) From the cubic spline deflection lines – (6) in Table 2

Figure 11 : Curvatures for unloaded states



a) From the raw deflection lines – Eq.(5) in Table 2 b) From the cubic spline deflection lines – (6) in Table 2

Figure 12 : Curvatures for loaded states

However, the derivative approximations show some error, perceptibly at the extremities of the curvatures. In normal condition of this simple beam, the curvature is annulled at the bearings; so it should be very weak near the bearings. Hence, as revealed in Figures 11-12, in no damaged states, the curvatures near the two extremities are not avoidable, even more important than in the middle of the beam. This error is accumulated through two times of derivative approximation, by adopting zero displacement at the two extremities of the deflections lines. This is only an approximation because in reality, the bearing is not only one point, it has significant dimension (Figure 1).

Nevertheless, the localization is satisfactory and the level of damage is well indicated, for both loaded and unloaded states. The results show that the detections based on the raw deflection lines and the interpolation are quite similar.

4 Conclusion

This paper has presented several techniques for damage detection from static data. By disposing a number of transducers along the structure, damage may be localized by watching the reordering of magnitude recorded in all transducers for every state. This reordering can be detected through the monitoring of the displacement increase due to loadings; of the residual deformation after each loading. Transducers that are more closed to damage will reveal clearer reordering.

Moreover, the establishment of deflection curves from static measurements is an effective means to localize damage. By this way, increase in flexibility may be observed around breaking points or important change of shape and amplitude of the deflection curves. Furthermore, in their slopes and especially curvatures, a sudden change allows indicating accurately the position of damage.

It reveals that this static monitoring is efficient even it does not require sophisticated and expensive equipment, the data processing is also straightforward what is practically feasible.

In order to avoid the including of plastic and irreversible deformations stayed after the first loading, the charging should be performed at least 2 times for each state and then use only the data from the second loading.

References

- Reynders E., De Roeck G. A local flexibility method for vibration-based damage localization and quantification. *Journal of Sound and Vibration*, Volume 329, Issue 12, pp. 2367–2383, 2010.
- Huth O., Feltrin G., Maeck J., Kilic N., and Motavalli M. Damage Identification Using Modal Data: Experiences on a Prestressed Concrete Bridge. *J. Struct. Eng. - ASCE*, 131(12), pp. 1898–1910, 2005.
- Nguyen V. H., Golinval J.-C. Damage localization and quantification for Beam-like Structures using Sensitivities of Principal Component Analysis Results. *Mechanical Systems and Signal Processing* 24, pp. 1831-1843, 2010.
- Khan M. A., Khan S. Z., Sohail W., Khan H., Sohaib M., Nisar S. Mechanical fatigue in aluminium at elevated temperature and remaining life prediction based on natural frequency evolution. *Fatigue & Fracture of Engineering Materials & Structures*, Volume 38, Issue 8, pp. 897–903, 2015.
- Inaudi D. Long-Term Static Structural Health Monitoring. *Structures Congress - ASCE*: pp. 566-577, doi: 10.1061/41130(369)52, 2010.
- Waltering M. Damage assessment of civil engineering structures and bridges using nonlinear dynamic characteristics. Dissertation PhD-FSTC-1-2009, University of Luxembourg, 2009.